JOURNAL OF AIRCRAFT
Vol. 32, No. 1, January–February 1995

Rolling Maneuver Load Alleviation Using Active Controls

Jessica A. Woods-Vedeler*
NASA Langley Research Center, Hampton, Virginia 23681
Anthony S. Pototzky†
Lockheed Engineering and Sciences Company, Inc., Hampton, Virginia 23666
and
Sherwood T. Hoadley‡
NASA Langley Research Center, Hampton, Virginia 23681

Rolling maneuver load alleviation (RMLA) has been demonstrated on the Active Flexible Wing wind-tunnel model in the NASA Langley Transonic Dynamics Tunnel (TDT). The objective was to develop a systematic approach for designing active control laws to alleviate wing loads generated during rolling maneuvers. Two RMLA control laws were developed that utilized outboard control surface pairs (leading and trailing edge) to counteract the loads and used inboard trailing-edge control surface pairs to maintain roll performance. Rolling maneuver load tests were performed in the TDT at several dynamic pressures including two below and one 11% above the open-loop flutter dynamic pressure. Above open-loop flutter, the RMLA system was operated simultaneously with an active Flutter Suppression System. At all dynamic pressures for which baseline results were obtained, torsion moment loads were reduced for both RMLA control laws. Results for bending moment load reductions were mixed; however, design equations developed in this study provided conservative estimates of load reduction in all cases.

Nomenclature

A = coefficient matrix defined by Eq. (3)
A_l = linear evaluation model coefficient matrix defined by Eq. (5)
B = control coefficient matrix defined by Eq. (3)
B_e = coefficient matrix for sin ϕ defined by Eq. (3)
C_{LOAD} = load output coefficient matrix defined by Eq. (8)
D_{LOAD} = load output control coefficient matrix defined by Eq. (8)
E_{LOAD} = steady-state load defined by Eq. (8)
g = acceleration due to gravity, in./s^2
I_{xx} = roll moment of inertia, 256.872 in.-lb-s^2
K_{com}, K_{TEI}, K_{TEO}, K_{LEO} = control system gains
L_p = rolling moment due to roll rate, in.-lb-s
L_{δ_i} = rolling moment due to deflection of control surface i, in.-lb/deg
l = distance between model c.g. and roll axis, in.
M = moment, in.-lb
M_0 = steady-state moment at 0-deg roll angle, in.-lb
M_{90} = steady-state moment at 90-degree roll angle, in.-lb
m = model mass, lb-s^2/in.
$\boldsymbol{u}$ = input vector
$\boldsymbol{x}$, $\dot{\boldsymbol{x}}$ = vector of state variables and its time derivative
$\boldsymbol{y}$ = output vector
$\boldsymbol{\delta}$ = vector of control surface deflections, deg
ϕ, $\dot{\phi}$, $\ddot{\phi}$ = roll angle and its time derivatives

Introduction

WITHOUT the use of active controls, it is necessary to provide passive solutions to the suppression of unfavorable aeroelastic response that result in increased structural stiffness of the wing and, thus, in increased weight. In the past 20 yr, the use of active controls has been investigated extensively as a means to control the aeroelastic response of aircraft. During this time, gust load alleviation using active controls has been successfully implemented on aircraft such as the Lockheed L1011[1] and the AIRBUS A320.[2] Flutter suppression has been demonstrated through wind-tunnel testing of a variety of aircraft,[3,4] and validated in flight testing on such aircraft as the B-52[5] and the F-4F.[6] Until recently, however, the use of active controls has not been successfully developed to alleviate wing loads generated during rolling maneuvers. Consequently, aircraft wings are still designed to support the increased loads generated during rolling maneuvers through added structural stiffness. The resultant increase in wing weight of the designed aircraft may be unnecessary if active controls technology is available to alleviate loads. Some past research has indicated the feasibility of rolling maneuver load alleviation (RMLA) using active controls.

During early testing of the Active Flexible Wing (AFW) wind-tunnel model in 1987,[7] maneuver load control systems

Presented as Paper 92-2099 at the Dynamic Specialists Conference, Dallas, TX, April 16–17, 1992; received May 10, 1992; revision received March 7, 1994; accepted for publication March 21, 1994.

*Aerospace Engineer, Structural Dynamics Branch, M/S 297. Member AIAA.
†Staff Engineer, Acoustics and Structures Dept., M/S 904. Senior Member AIAA.
‡Senior Aerospace Engineer, Aeroelasticity Branch, M/S 340. Associate Fellow AIAA.

were demonstrated for longitudinal motion of AFW. The concepts involved reducing a wing-root bending moment during pitch maneuvers through the use of angle-of-attack feedback, scheduled wing cambering using control surface deflections, and bending-moment strain gauge feedback. Significant reductions in bending moment were achieved. Based on this success, the possibility of designing a control law to actively reduce wing loads during rolling maneuvers was considered feasible. During the same 1987 test, an active roll control system (ARC) was developed to maneuver the model to a commanded roll angle position at a specified roll rate. During evaluation of this control law, the potential for using active controls to redistribute wing loads during rolling maneuvers was recognized. However, a systematic approach for designing control laws to reduce wing loads during rolling maneuvers was not developed.

The intent of the current research was to develop RMLA control laws that would reduce dynamic wing loads during fast rolling maneuvers using digitally implemented active controls. A systematic synthesis approach is defined for developing RMLA control laws. Using this approach, two RMLA control laws were developed for the AFW wind-tunnel model, and results from controlled rolling maneuvers performed in the Langley TDT, both below and above (using a flutter suppression control law operating simultaneously with RMLA) the open-loop flutter boundary are presented.

RMLA Design Concept

The original objective of the research presented in this article was to develop an active RMLA control laws design that would attempt to alleviate both bending and torsion moment wing loads during fast rolling maneuvers. Specifically, the basic RMLA design concept employed herein involves designing controls laws that minimize the peak deviation of the wing loads during a rolling maneuver from their steady-state value prior to the maneuver. Partial motivation for choosing the peak deviation from the steady-state value as a basis of load reduction is due to the large artificially induced static loads that result from the model being constrained to roll about a sting in the wind tunnel. This would not be the same for a real aircraft in flight. The basis for RMLA design in that case could be, e.g., the loads about the load point induced by gravity. However, the systematic synthesis approach defined in this article for developing RMLA control laws would still be the same. In addition to reducing peak incremental loads, the control laws were designed to meet specified "time-to-roll" performance requirements and certain stability-margin requirements. Also included in the control law design was the requirement that the control laws be implemented by a digital controller.

To evaluate load reduction, it is necessary to compare loads sustained during a rolling maneuver employing an active RMLA control law against those of a baseline rolling maneuver having the same time-to-roll performance. Consequently, a baseline control law had to be designed that met the same time-to-roll performance and stability-margin requirements as the RMLA control laws. The baseline control law, described in this article, served as a measuring stick against which to calculate load reductions achieved by each of the RMLA control laws for specified rolling maneuvers.

The AFW concept was developed at Rockwell International Corporation in the mid1980s.[7] This concept exploited, rather than avoided, wing flexibility to provide weight savings and improved aerodynamic performance. Details of the AFW model including the model construction and rotatable sting mount and tip ballasts are provided in an accompanying summary paper and Refs. 7–9. The control laws described in this document were implemented during wind-tunnel testing using the digital controller system (DCS), and the details of the controller are presented in Ref. 10.

Plant Equations

As stated earlier, the ARC system,[11] designed to minimize control surface deflections during rolling maneuvers, was experimentally evaluated during the 1987 AFW wind-tunnel test. The assumption made in that study was that the frequency content of the commanded input was well below the frequency of the first flexible mode so that the flexible modes would not be excited by the motion of the control surfaces designed for rolling maneuver load control. Because only rigid-body motion was used in the design of the ARC system, and because analytical and experimental results compared well in this previous study, it was considered sufficient to design RMLA control laws in the present study using only the rigid-body roll equation. Consequently, the RMLA control laws presented herein used only the rigid-body roll equation and load equations in the design model.

The rigid-body roll equation of motion for the open-loop wind-tunnel model used in both this study and that of Ref. 11 is described by Eq. (1):

$$I_{xx}\ddot{\phi} - L_p\dot{\phi} + mgl\sin\phi = \sum_{i=1}^{6} L_{\delta_i}\delta_i \tag{1}$$

Many of the coefficients and variables used in the equation were originally defined in Ref. 12; however, Eq. (1) differs in two ways from those of Ref. 12: control-surface rate derivatives have been neglected, and the quantity $mgl \sin \phi$, referred to herein as the pendulum term, has been added. This pendulum term quantity is necessary because the c.g. of the wind-tunnel model is a distance l below the roll axis of the model. This term is not representative of real aircraft, and causes Eq. (1) to be nonlinear. The nonlinear term can be linearized for small roll angles by the fact that $\sin\phi \approx \phi$ (ϕ in radians); however, for the large roll angles experienced during wind-tunnel testing, the small angle assumption is violated. Nevertheless, this assumption was still considered reasonable in order to obtain estimates of behavior using a linearized model that includes the pendulum effect, and to simplify the design of control laws, a linearized model of the plant was desired. To this end, three sets of plant equations were developed. The first was comprised of linearized state-space equations with the nonlinear pendulum term included explicitly, the second included a linearized pendulum term in the linearized state-space equations, and the third was a linearized state-space design model that contained no pendulum term. The first two were simulation models used for evaluation of analytical results; the last was used for the actual RMLA control law design. A discussion of the techniques used to identify plant parameters for the plant equations from experimentally obtained data is presented in Ref. 13. A study of the relative moment contribution of the pendulum term with respect to the moment due to control surface deflections was performed to justify the exclusion of the pendulum term in the design model. The details of this study are also presented in Ref. 13.

Nonlinear Model

Equation (1) can be expressed in state-space form as

$$\dot{\boldsymbol{x}} = A\boldsymbol{x} + B\boldsymbol{u} + B_e \sin\phi \tag{2}$$

where

$$\boldsymbol{x} = \{\dot{\phi},\ \phi\}^T$$

$$\boldsymbol{u} = \{\delta_i\}$$

$$A = \begin{bmatrix} (L_p/I_{xx}) & 0 \\ 1 & 0 \end{bmatrix}$$

$$B = \{(L_{\delta_i}/I_{xx}) \quad 0\}^T$$

for $i = \mathrm{LEO}_L, \mathrm{TEO}_L, \mathrm{TEI}_L, \mathrm{LEO}_R, \mathrm{TEI}_R$

$$B_e = \{-(mgl/I_{xx}) \quad 0\}^T \tag{3}$$

Linear Model

Equation (2) is linearized by assuming $\sin\phi \approx \phi$, resulting in the following linearized model:

$$\dot{x} = Ax + Bu + B_e\phi = A_l x + Bu \tag{4}$$

where

$$A_l = \begin{bmatrix} (L_p/I_{xx}) & -(mgl/I_{xx}) \\ 1 & 0 \end{bmatrix} \tag{5}$$

and x, u, and B are defined as in Eqs. (2) and (3).

Design-Model Plant Equations of Motion

Simulation studies performed[13] showed that the contribution to total rolling moment of the pendulum term due to mass eccentricity relative to control surface deflections was not significant during faster rolling maneuvers. As a result, the pendulum term was removed from Eq. (2) to form the design-model linearized plant equations in state-space form:

$$\dot{x} = Ax + Bu \tag{6}$$

Plant Output Equations

Besides defining the roll angle and roll rate as output quantities in the equations of motion, additional outputs of interest for RMLA control law design are the torsion and bending moments. The load equations, along with roll angle and roll rate, are expressed in linearized state-space output equations describing the roll rate, roll angle, and model loads experienced during rolling maneuvers by Eq. (7)

$$y = \begin{Bmatrix} \{\dot{\phi}\ \phi\}^T \\ y_{\text{LOAD}} \end{Bmatrix} = \begin{bmatrix} I_2 \\ C_{\text{LOAD}} \end{bmatrix} x + \begin{bmatrix} \{0\ 0\}^T \\ D_{\text{LOAD}} \end{bmatrix} u + \begin{bmatrix} \{0\ 0\}^T \\ E_{\text{LOAD}} \end{bmatrix} \tag{7}$$

where

$$y_{\text{LOAD}} = \{M_i\}$$

$$I_2 = \begin{bmatrix} 1 & 0 \\ 0 & 1 \end{bmatrix}$$

$$C_{\text{LOAD}} = \begin{bmatrix} \dfrac{\partial M_i}{\partial \dot{\phi}} & \dfrac{\partial M_i}{\partial \phi} \end{bmatrix}$$

$$0 = [0\ 0\ 0\ 0\ 0\ 0]$$

$$D_{\text{LOAD}} = \begin{bmatrix} \dfrac{M_i}{\partial \delta_j} \end{bmatrix}$$

$$E_{\text{LOAD}} = \{M_{0_i}\} \tag{8}$$

for

$$i = t_{\text{LI}}, t_{\text{LO}}, t_{\text{RI}}, t_{\text{RO}}, b_{\text{LI}}, b_{\text{LO}}, b_{\text{RI}}, b_{\text{RO}}$$

$$j = \text{LEO}_L, \text{TEO}_L, \text{TEI}_L, \text{LEO}_R, \text{TEO}_R, \text{or TEI}_R$$

Equations (7) and (8) define the plant-output equations for both the evaluation and design models. The parameters for these equations were derived experimentally.[13] The terms in E_{LOAD} are either a steady-state torsion moment or bending moment at one of the inboard or outboard locations of the left or right wing. Inertial loads were not modeled.

RMLA Control Law Synthesis

The approach used in this study to develop RMLA control laws was based on observations of how incremental loads varied during simulated rolling maneuvers and how control surface deflections affected these loads. The linear design-model described by Eq. (6) above was used as the basis of the RMLA design. Additionally, output equations described by Eqs. (7) and (8) formed the basis of the load calculations; however, for the design model, the steady-state loads M_{0_i}, were assumed to be 0 ($E_{\text{LOAD}} = 0$), meaning that the incremental loads were assumed to equal to the output loads. For other elements in the design model, the experimentally-derived parameters were used.

The basic design objective for RMLA was to reduce incremental loads generated during a rolling maneuver with no roll performance penalty. As previously mentioned, this meant developing active RMLA control laws that would attempt to alleviate both bending and torsion moment wing loads during fast rolling maneuvers. Some preliminary studies using results of control surface roll and load effectiveness from earlier 1989 wind-tunnel tests showed that the trailing-edge inboard pair of control surfaces generated the largest rolling moments; however, the outboard control surfaces demonstrated a more substantial ability to affect incremental loads during rolling maneuvers. This implied that the outboard surfaces could be deflected a limited amount during a maneuver in order to alleviate loads, and any roll performance lost due to this actuation of outboard control surfaces could be regained by increased deflections of the trailing-edge inboard (TEI) control surfaces. From initial simulation studies, it was found that bending and torsion moment loads were highly coupled to each other and to the angular deflections of the control surfaces. This inherent coupling of the loads indicated that simplifying the control objective by targeting the reduction of a single type of load was plausible. Another simulation study showed that when using the inboard control surfaces to roll the model, torsion-moment peak incremental loads were significantly larger relative to their steady-state values than the respective bending-moment loads. Based on these preliminary results, the original RMLA objective was modified to target reductions of only the peak incremental torsion moments rather than those of both the torsion and bending moments, making the design effort significantly simpler. This modification meets much of the original research objective, although care must be taken that the tradeoff (in this case, possible increases in the peak incremental bending moments) is not too severe.

The RMLA control law synthesis procedure used herein involves four steps that are outlined as follows:

Step 1. Evaluate Control Surface Load Effectiveness

Evaluate the ability of each control surface to effect change loads during rolling maneuvers.

Right and left control surfaces were deflected differentially with a positive deflection to a control surface pair being defined so that the left control surface was deflected upward (negative) and the right downward (positive). Using a preliminary design model, negative (differential) deflections of both outboard control surface pairs were found to cause decreases in outboard incremental bending loads. Similar results were obtained for the inboard incremental bending loads and inboard incremental torsion loads; however, only negative deflections of the trailing-edge outboard (TEO) control surfaces resulted in decreases in outboard incremental torsion loads. This implied that the TEO control surfaces should be the most effective in reducing all incremental loads. Uncertainty, however, of the preliminary math model for this study led to the decision to design control laws that used both sets of outboard control surfaces, independently, as a first attempt in RMLA control.

Step 2. Determine Potential Control Law Form

Establish effective control surface combinations and a feedback control law form that can potentially reduce dynamic loads.

Based on studies discussed previously, it was decided to develop two RMLA control laws which 1) actuated the TEI

control surfaces in the positive direction differentially to effect roll, 2) actuated outboard control surface pairs (either leading or trailing edge) in the negative direction differentially to reduce peak incremental torsion-moment loads, and 3) adjusted the control surface deflections based on the roll rate. The RMLA control law consisting of a gain-feedback structure with low-pass filters as illustrated in Fig. 1 was selected as the basic RMLA control law structure to be used for this study. As mentioned, the structure includes roll-rate feedback to the TEI, leading-edge outboard (LEO), and TEI control surface pairs. Left and right wing control surfaces in each pair are deflected differentially. In addition to the roll-rate feedback, the roll-rate command, describing the desired roll-rate performance, is sent to the TEI control surface pair to effect roll.

Since the first flexible mode frequency was above 7 Hz, a 8.75-Hz low-pass filter was included in each loop of the system in order to minimize the effect of the RMLA control laws on the flexible modes that would be present while testing and to smooth the input command. As indicated in the figure, there were a command input gain, labeled K_{com}, and feedback gains to TEI, TEO, and LEO, control surfaces labeled K_{TEI}, K_{TEO}, and K_{LEO}, respectively.

Step 3. Determine Control Law Gains

Iterate control system gains for various control surface combinations to determine a set which effectively reduces targeted dynamic loads during specified rolling maneuvers.

Three control laws, referred to herein as A, B, and Baseline, were developed using experimentally-derived equations of motion and plant output equations. Each was designed to meet test objectives at a design dynamic pressure of 150 psf and corresponding Mach number of 0.33. The control laws were then evaluated using the design model for $q = 250$ psf and Mach of 0.44, and gains were iterated until torsion moments were effectively reduced. Control law A was defined by roll-rate feedback to the TEO control surface pair and to the TEO control surface pair with gains $K_{com} = 0.35$, $K_{TEI} = -0.0625$, $K_{TEO} = -0.0384$, and $K_{LEO} = 0$. Control law B was defined by roll-rate feedback to the TEO control surface pair and to the LEO control surface pair where $K_{com} = 0.30$, $K_{TEI} = -0.0667$, $K_{TEO} = 0$, and $K_{LEO} = 0.0356$. Finally, the Baseline control law was defined by roll-rate feedback to the TEI control surface pair only with $K_{com} = 0.35$, $K_{TEI} = -0.0500$, $K_{TEO} = 0$, and $K_{LEO} = 0$.

Step 4. Determine Control System Stability and Robustness

After iterating for a set of control system gains, check that stability margins are adequate.

System stability was determined analytically for each closed-loop system at the two design conditions, $q = 150$ and 250 psf, using each of the three control laws defined above. For the stability analyses discussed herein, the parameters from the experimentally defined models were used for the equations, and the roll-rate command, $\dot{\phi}_{com}$ was assumed to be 0.

Each of the three control laws presented was stable. Furthermore, once system stability is established, stability margins can be determined using the method described in Ref. 14. With this method, the regions of guaranteed stability over a system's operating frequency range can be predicted by plotting the minimum singular value of the linear-system return-difference matrix on the universal gain and phase margin diagram. Stability margins were considered adequate for these control laws.[13]

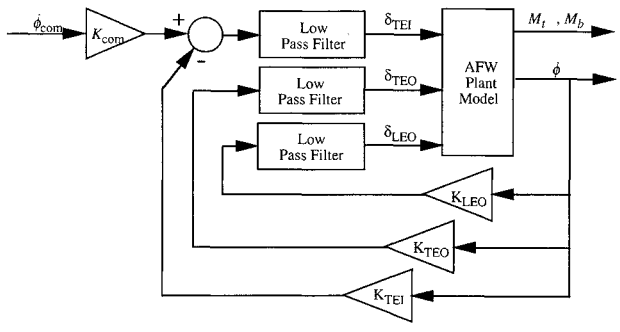

Fig. 1 RMLA control law structure.

Test Procedures for RMLA Performance Evaluation

Initially, control laws A and B and the Baseline control law were tested at tunnel test conditions having dynamic pressures of 150, 200, and 250 psf, and Mach numbers of 0.33, 0.39, and 0.44, respectively. The model was configured for each of these tests so that open-loop flutter would not be incurred. Each RMLA-controlled rolling maneuver commenced with the model positioned at 90-deg roll angle, and was terminated shortly after the model rolled through 0-deg roll angle. Maneuvers at $q = 150$ and 200 psf were performed with the tip ballast coupled; however, those at $q = 250$ psf were performed with the tip ballast decoupled in order to raise the open-loop flutter dynamic pressure above the testing dynamic pressure.

Rolling maneuvers were also performed above the open-loop flutter dynamic pressure at $q = 250$ and 260 psf with the tip ballast coupled. For these maneuvers, RMLA control law B was implemented simultaneously with an active flutter suppression system (FSS) using the control law described in Ref. 15. During these multiple-function maneuvers, the rolling maneuvers commenced with the model positioned at 70-deg roll angle instead of 90 deg, and were terminated as the model rolled through −20 deg. Because the steady-state plus dynamic loads at 90 deg (prior to the rolling maneuver) were too close to the preselected load limits of the trip system for the wind-tunnel model, these changes were made to allow the multifunction rolling maneuver tests to be conducted in a dynamic load range where the loads were less likely to trigger the trip system.

Figure 5 of Ref. 10 (also Fig. 16 of the accompanying paper on the AFW digital controller) provides a description of how the RMLA controllers were commanded during testing and how the roll-rate commands were implemented on the digital controller. It should be mentioned that in order to simplify the control law design process, the rolling maneuver load control laws were only designed to reduce loads for the portion of the maneuver prior to the point where the roll-rate commands were ramped off, identified as t_T in the figure, and comparison of the results described herein are for this design region only.

For both the single-function RMLA testing and the multiple-function testing, rolling maneuvers were repeated at each test point for several different roll-rate commands to assure that data obtained was in the performance range of interest.

Data Reduction for RMLA Performance Evaluation

Before describing the results obtained from wind-tunnel testing, a brief discussion of the data reduction used to evaluate the RMLA performance is necessary. First, peak incremental loads had to be extracted from test data for each rolling maneuver performed. Four incremental loads were examined: 1) outboard incremental bending moment, ΔM_{b_O}, 2) inboard incremental bending moment ΔM_{b_I}, 3) outboard incremental torsion moment ΔM_{t_O}, and 4) inboard incremental torsion moment ΔM_{t_I}. These incremental loads are defined for $j = O$ (outboard) or I (inboard) by

$$\Delta M_{b_j}(t) = \tfrac{1}{2}[(M_{b_{R_j}} - M_{90_{b_{R_j}}}) - (M_{b_{L_j}} - M_{90_{b_{L_j}}})](t) \quad (9a)$$

$$\Delta M_{t_j}(t) = \tfrac{1}{2}[(M_{t_{R_j}} - M_{90_{t_{R_j}}}) - (M_{t_{L_j}} - M_{90_{t_{L_j}}})](t) \quad (9b)$$

and peak incremental loads for all the rolling maneuvers were computed from the experimental data using

$$\overline{\Delta M_{b_j}} = \max_t |\Delta M_{b_j}(t)| \tag{10a}$$

$$\overline{\Delta M_{t_j}} = \max_t |\Delta M_{t_j}(t)| \tag{10b}$$

Controlled rolling maneuvers had different performance times than the baseline maneuvers, and time did not permit performing additional maneuvers to obtain the same performance times. Because it was necessary to compare the RMLA maneuvers with baseline maneuvers having the same performance times, peak incremental loads obtained for baseline maneuvers were interpolated as a function of performance time to correspond to performance times equal to those achieved during RMLA-controlled maneuvers.

Results and Discussion

Experimental results obtained using Eqs. (9) and (10) were calculated for all RMLA-controlled rolling maneuvers and the baseline-rolling maneuvers. Discussion and comparisons of each of the resulting incremental loads and peak incremental loads are too numerous to present in this article for all maneuvers and test conditions; however, the resulting load alleviation achieved using RMLA control laws A and B are presented and the performance of the two control laws are compared. Finally, an evaluation of the multiple-function performance of RMLA control law B implemented with a flutter suppression control law is presented.

Time History Comparisons of Incremental Loads

Some typical time-history results obtained during wind-tunnel evaluation for RMLA control law B are shown in Fig. 2 comparing incremental loads during a rolling maneuver controlled by control law B with those from a corresponding baseline maneuver having nearly the same performance time-to-roll 90 deg. Since the performance times are nearly the same, comparison can be made between the actual RMLA and baseline load time histories rather than with only interpolated peak incremental loads. The rolling maneuver was a 90- to 0-deg roll at a dynamic pressure of 200 psf having performance times of 0.645 s for control law B, and 0.65 s for the Baseline control law. Roll-rate and roll-angle time histories are shown in Figs. 2a and 2b, respectively. A vertical dashed line indicates the approximate point in time at which the RMLA-controlled rolling maneuver was considered terminated, and the roll-rate command ramped off.

Decreases in incremental torsion moments are observed in Figs. 2c and 2d for most of the rolling maneuver from 90 to 0 deg. In fact, there is a substantial decrease in peak incremental outboard and inboard torsion moments from 495.1 and 1565 in.-lb, respectively, at 0.49 s for the baseline control law to 265.6 and 885.8 in.-lb, respectively, at 0.4 s for control law B. This substantial reduction in peak incremental torsion

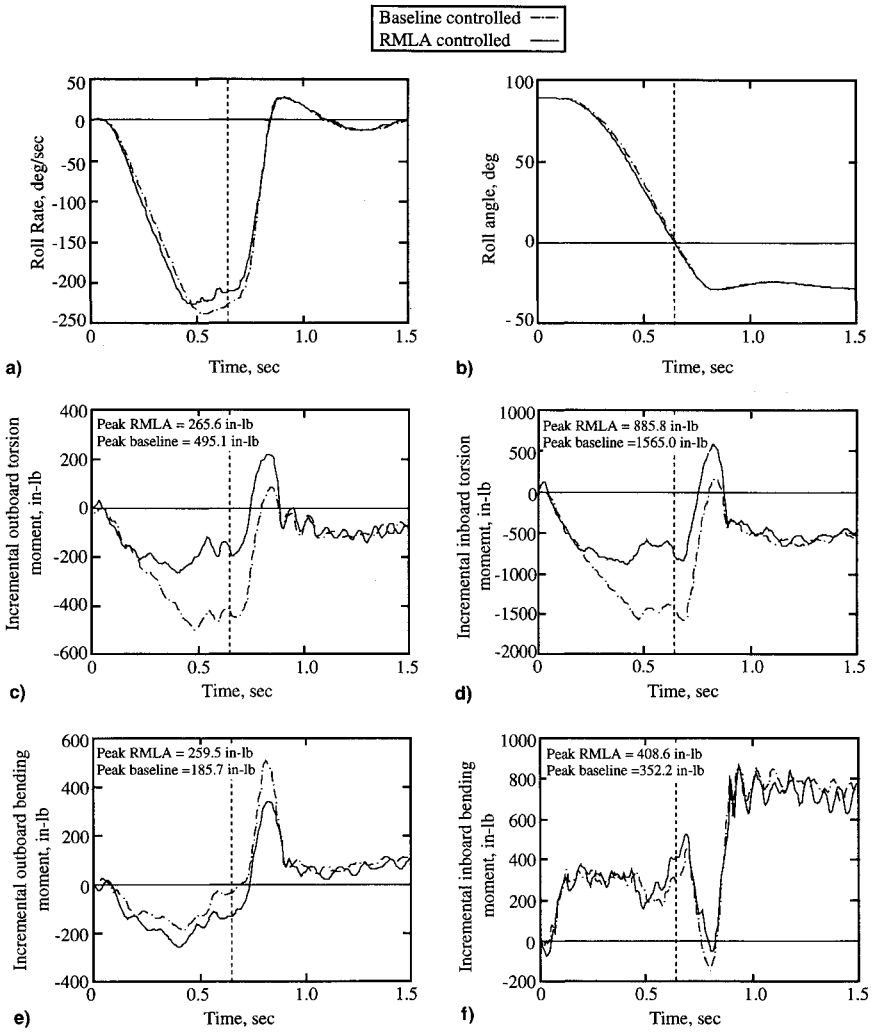

Fig. 2 RMLA control law B controlled maneuver loads compared to baseline loads at q = 200 psf having performance times equal to 0.645 and 0.65, respectively: a) roll rate, b) roll angle, and the incremental c) outboard torsion, d) inboard torsion, e) outboard bending, and f) inboard bending moments.

moments using leading-edge controls was not predicted with a preliminary design study; however, this reduction with respect to the baseline rolling maneuver is typical of all the RMLA-controlled rolling maneuvers for both control laws.

Similar comparisons for the incremental bending moments (Figs. 2e and 2f) indicate increases in the peak incremental load for the outboard and inboard bending moments, but all peak incremental loads are nearly the same for the RMLA-controlled maneuver. In fact, one incremental load which is significantly larger than all the others for the baseline maneuver, namely the inboard torsion moment, is brought within the same level of load as all the others. Since the design criteria did not include the peak incremental bending moments, it is not surprising to see an increase in these as a result of lowering the peak incremental torsion moments.

Similar decreases and increases in incremental loads were observed for control law A, except there were more substantial increases in incremental outboard bending moment for A than B. The significance of the load increases in order to evaluate the severity of tradeoff between decreases and increases in incremental loads is addressed in the next two sections.

Typical Load Alleviation Results

The bar graphs shown in Fig. 3 summarize the percent changes in peak incremental loads relative to the baseline for both control law B, shown in Fig. 2, and a corresponding maneuver for control law A. The first bar in each group presents the baseline results; the second and third, the changes corresponding to control law A and B, respectively. The figure shows that the peak outboard incremental torsion moment is reduced by 27.4% relative to the baseline case and peak inboard incremental torsion moment is reduced by 52.3% for control law A. There are corresponding decreases of 46.4 and 43.4% for control law B. However, there are increases in bending moments for each control law. Specifically, there are increases of 14.7 and 16.0% in the peak value of inboard incremental bending moment. Peak outboard incremental bending moment for control law A, however, is shown to increase by approximately two and half times with respect to the baseline, whereas that of control law B is 39.7%.

In order to gauge the significance of these results for each load, a comparison can made between changes in peak incremental loads and the static-load limits. It can be determined that the percentage increase of 16.0% in peak inboard incremental bending moment shown in the figure for control law B is less than 0.3% of the minimum inboard bending-moment static-load limit. Similarly, the percentage increase in peak outboard incremental bending moment represents less than 2.1% of the minimum outboard bending moment static load limit. On the contrary, the percentage decreases in peak outboard and inboard incremental torsion moments represent larger percentages, namely, 16.1 and 7.6% of their respective torsion moment static-load limits.

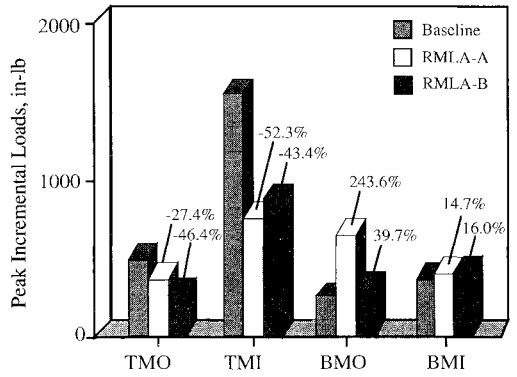

Fig. 3 Change in peak incremental loads for two RMLA-controlled maneuvers having performance times nearly the same as the baseline control law at q = 200 psf.

The corresponding changes in peak incremental loads for control A are −9.5 and −9.2% in the peak incremental outboard and inboard torsion moments, respectively, but increases of 12.8 and 0.3% for outboard and inboard bending moments. For both control laws, the decreases in the outboard torsion moment are considered to be significant since the amount of load alleviation represents a substantial portion of each wing's capacity to support outboard torsion moments. The small percentage increases in the bending moments due to control law B are considered to be an inconsequential tradeoff; however, the increase for control law A warrants further investigation.

Overall Analysis of Experimental Results

This section provides an overall analysis of all the rolling maneuvers performed in the TDT using two RMLA control laws described herein and the baseline control law. The same trends as indicated in the previous comparisons occurred between all the RMLA-controlled maneuvers and the baseline maneuvers. The peak incremental loads were calculated from the experimental data using Eq. (10) for all the rolling maneuvers, and these results are presented in Table 1. As can be seen in the table, RMLA-controlled rolling maneuvers had different performance times than the baseline maneuvers, and time did not permit performing additional maneuvers to obtain exactly the same performance times. In order to compare results, peak incremental loads for baseline maneuvers were interpolated to correspond to performance times equal to those for RMLA-controlled maneuvers. These calculations are presented in Table 2, and interpolated values were used for all subsequent discussions.

The results in Table 2 show that the peak incremental torsion moments are decreased in every case for both control laws. This is consistent with the control law design criteria. Since the results for bending moments are mixed, and in some cases, as indicated in the previous section, might represent too great a tradeoff penalty, it is necessary to evaluate these results further. Two ways to look at the relative importance of the peak incremental change in load is to compare it with initial steady-state loads at 90-deg roll angle and minimum static load limits.

Figure 4 shows graphically percentage changes in the peak incremental loads between all RMLA-controlled maneuvers and the baseline maneuvers with respect to the average (left and right) steady-state loads for a dynamic pressure of 200 psf. The percent changes are plotted with respect to performance time-to-roll 90 deg. Each percentage shown in the figure is in terms of its respective initial steady-state load value so that relative importance of the change with respect to the initial load can be assessed more easily. Increasing time implies slower rolls and less incremental change. For both RMLA control laws, the rolling maneuvers produced both positive and negative percentage changes. A negative percentage indicates a decrease in the incremental load from the peak baseline incremental loads for either control law. Several observations can be made.

For both control laws A and B, Fig. 4 shows load reductions of the inboard and outboard torsion moments. These reductions ranged from about 21% at a dynamic pressure of 150 psf for control law A. to as much as 140% at 250 psf for control law B. In general, the reductions tend to increase with increased dynamic pressure. In most cases, for all three dynamic pressures (150, 200, and 250 psf) rolling the model slower resulted in less reduction in the peak incremental torsion moments due to decreased overall loads. It can be seen from both bar graphs that reductions for outboard torsion moment are greater for control law B using the LEO control surfaces for load reduction, and those for inboard torsion moment were greater for control law A using the TEO control

Table 1 Peak incremental loads from experimental data for baseline and two RMLA control laws

Dynamic pressure q, psf	Control law	Time-to-roll 90 deg, s	Peak incremental loads TMO, in.-lb	TMI, in.-lb	BMO, in.-lb	BMI, in.-lb
150	Baseline	0.670	391.6	1206.0	180.9	313.6
150	Baseline	0.705	343.7	1102.0	164.9	342.2
150	Baseline	0.825	304.3	988.9	118.1	413.0
200	Baseline	0.575	580.0	1829.0	282.1	423.3
200	Baseline	0.650	495.1	1565.0	185.7	352.2
200	Baseline	0.805	394.1	1256.0	130.8	459.9
250	Baseline	0.555	719.1	2239.0	312.5	414.7
250	Baseline	0.645	636.2	1803.0	269.0	363.1
250	Baseline	0.665	544.4	1617.0	244.8	460.4
250	Baseline	0.795	506.7	1497.0	168.4	429.1
150	A	0.675	308.4	679.5	493.8	313.3
150	A	0.695	300.7	699.5	488.4	361.8
150	A	0.805	263.4	523.2	415.4	279.2
200	A	0.635	376.3	628.5	731.1	442.7
200	A	0.660	359.6	747.1	638.0	403.8
200	A	0.770	302.1	570.6	551.3	341.2
250	A	0.600	405.0	776.0	915.4	560.0
250	A	0.640	394.4	741.1	825.2	590.6
250	A	0.735	335.2	615.9	696.8	486.6
150	B	0.650	251.1	858.1	250.8	334.6
150	B	0.675	225.6	787.2	234.4	307.6
150	B	0.780	178.0	684.7	164.8	455.7
200	B	0.615	279.0	1064.0	294.3	450.1
200	B	0.645	265.6	885.8	259.5	408.6
200	B	0.740	205.1	772.9	217.7	547.3
250	B	0.630	293.4	909.1	328.0	366.2
250	B	0.740	218.0	821.1	230.1	498.4
250	B	0.770	226.4	700.4	240.5	531.0

Table 2 Comparison of peak incremental loads for RMLA controls laws with interpolated baseline maneuver loads

Dynamic pressure q, psf	Time-to-roll 90 deg, s	Peak incremental loads TMO Baseline, interpolated	TMO Control A	TMI Baseline, interpolated	TMI Control A	BMO Baseline, interpolated	BMO Control A	BMI Baseline, interpolated	BMI Control A
a) RMLA control law A[a]									
150	0.675	384.8	308.4	1191.1	679.5	178.6	493.8	317.7	313.3
150	0.695	357.4	300.7	1131.7	699.5	169.5	488.4	334.0	361.8
150	0.805	310.9	263.4	1007.8	523.2	125.9	415.4	401.2	279.2
200	0.635	512.1	376.3	1617.8	628.5	205.0	731.1	366.4	442.7
200	0.660	488.6	359.6	1545.1	747.1	182.2	638.0	359.1	403.8
200	0.770	416.9	302.1	1325.8	570.6	143.2	551.3	435.6	341.2
250	0.600	677.7	405.0	2021.0	776.0	290.8	915.4	388.9	560.0
250	0.640	640.8	394.4	1827.2	741.0	271.4	825.2	366.0	590.6
250	0.735	524.1	335.2	1552.4	615.9	203.7	696.8	443.5	486.6

Dynamic pressure q, psf	Time-to-roll 90 deg, s	Peak incremental loads TMO Baseline, interpolated	TMO Control B	TMI Baseline, interpolated	TMI Control B	BMO Baseline, interpolated	BMO Control B	BMI Baseline, interpolated	BMI Control B
b) RMLA control law B[a]									
150	0.650	419.0	251.1	1265.4	858.1	190.0	250.8	297.3	334.6
150	0.675	384.8	225.6	1191.1	787.2	178.6	234.4	317.7	307.6
150	0.780	319.1	178.0	1031.3	684.7	135.7	164.8	386.5	455.7
200	0.615	534.7	279.0	1688.2	1064.0	230.7	294.3	385.4	450.1
200	0.645	500.8	265.6	1582.6	885.8	192.1	259.5	356.9	408.6
200	0.740	436.5	205.1	1385.6	772.9	153.8	217.7	414.7	547.3
250	0.630	650.0	293.4	1875.7	909.1	276.2	328.0	371.7	366.2
250	0.740	522.7	218.0	1547.8	821.1	200.7	230.1	442.3	498.4
250	0.770	514.0	226.4	1520.1	700.4	183.1	240.5	435.1	531.0

[a]Percentages differ from corresponding results in Table 1 because interpolated values are used for the baseline.

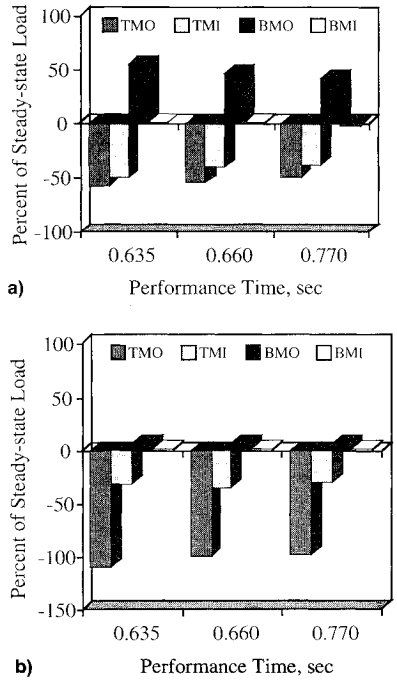

Fig. 4 Percent change in peak incremental load between baseline loads and RMLA-controlled loads relative to steady-state loads at beginning of maneuver: control law a) A, q = 200 psf and b) B, q = 200 psf.

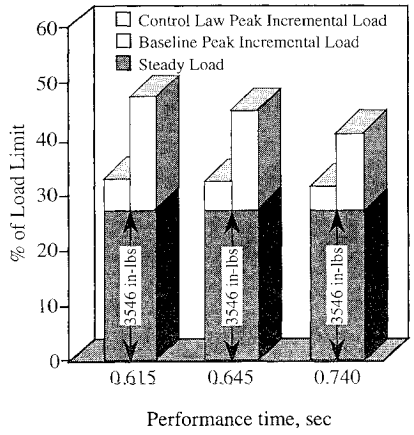

Fig. 5 Outboard bending moment comparison of steady plus peak incremental load relative to static load limits for baseline control law and control law A at q = 200 psf.

surfaces. These results are typical for all test points. Furthermore, the reductions in peak incremental torsion moments combined outweigh the combined increase in peak incremental bending moments in all cases for both control laws.

The only issue still to be resolved is whether the increase in peak incremental outboard bending moment represents too severe a tradeoff penalty. To answer this question, percent changes relative to corresponding minimum static load limits were also calculated. Results tend to indicate that in the case of control law A, in which peak incremental bending moments decidedly increase, the increase is not significantly large with respect to the load limits. To verify this further, a comparison of the peak incremental baseline load, peak incremental RMLA-controlled load, and the initial steady-state load relative to the static load limits was performed. The only increase in incremental load due to RMLA control of significant interest is that for outboard bending moment, and results for this load at q = 200 psf are plotted in Fig. 5. This figure depicts the relative percent difference between the RMLA-controlled load and the baseline in terms of the load limit percentages using an accumulative bar graph. The percentage of steady-state load relative to the static load limit is shown as a dark vertical bar of constant height for each load. The percentage change in peak incremental load relative to the static load limit is added to this. The RMLA-controlled load is plotted to the right of the baseline load. It can be seen that even in this case, the total load change is less than 50% of the static load limit. In fact, total loads are less than 50% for all RMLA-controlled loads (not shown) for this dynamic pressure. Furthermore, very little change in inboard bending moment is effected from the use of either LEO or TEO control surfaces.

Summary of Experimental Results

To summarize the results of the previous discussion, in general, control law B, which used the LEO control surface pair, resulted in higher reductions in outboard incremental torsion moments than control law A. The reverse is true for the inboard incremental torsion moments. This suggests that, for the AFW wind-tunnel model, use of the LEO control surface pair is more effective at reducing the outboard incremental torsion moments, whereas the use of the TEO control surface pair is more effective in decreasing inboard incremental torsion moments. In both cases, the targeted design goal, namely, reducing peak incremental torsion moments, was substantially met. Control laws A and B differed more significantly in how peak incremental bending moments were affected during rolling maneuvers; however, in all test cases, the RMLA-controlled load plus the corresponding initial steady-state load did not exceed 57% of the static load limit.

In general, control law B demonstrated the better overall RMLA characteristics relative to the limit loads for the combinations of Mach number and dynamic pressure tested. Substantially large reductions were achieved in both inboard and outboard incremental torsion moments without significant increases in incremental bending moments, confirming initial perceptions that only torsion moment needs to be targeted for load reduction in designing an RMLA control law. Since reductions relative to static load limits are most significant for outboard torsion moments and increases in bending moments for this control law were not severe, control law B is considered to be the more effective of the two for rolling maneuver load alleviation. At higher Mach numbers and dynamic pressures, hinge-moment loads on the leading-edge surface could become excessive using only roll-rate feedback, and the actuators might saturate. In this case, not explored with this model, a control law using only the trailing-edge control surfaces or one using hinge-moment feedback might be prudent. For good performance at all conditions, control laws using combinations of both leading- and trailing-edge control surface pairs with gain scheduling should be explored.

Multiple-Function Control Law Performance Results

Successful rolling maneuvers 6 and 11% above the open-loop flutter dynamic pressure were achieved, experimentally, using a flutter suppression control law[15] implemented on the digital controller in conjunction with RMLA control law B. Flutter did not occur during these maneuvers, indicating the flutter suppression control law was suppressing the instability during roll without any significant interference. A qualitative evaluation of load reduction above open-loop flutter cannot be made because time did not permit corresponding baseline data to be obtained. However, based on comparisons of incremental loads with the FSS control law operating at subcritical dynamic pressures for which comparable baseline data is available, namely at q = 150 and 200 psf, it is likely that incremental load reduction also occurred for this test condition. Since trip limits were not incurred during these rolling maneuvers, it can at least be stated that control law B did not induce excessive incremental loads during rolling maneuvers for which it was designed above the open-loop flutter dynamic pressure.

Concluding Remarks

This report provides a systematic synthesis methodology to design RMLA feedback control laws. Using the methodology presented, two relatively simple RMLA control laws, referred to herein as A and B, were designed and implemented on a digital control computer. The two control laws differed in whether LEO or TEO control surfaces were used to alleviate load. These control laws were experimentally evaluated and shown to effectively and reliably reduce incremental torsion loads on the AFW wind-tunnel model in Transonic Dynamics Tunnel (TDT). In addition, it was demonstrated through wind-tunnel tests that a digital control computer can be used with great versatility to perform a multifunction task such as suppressing flutter and reducing loads during rolling maneuvers. The following is a list of the accomplishments achieved in this research:

1) Load alleviation during controlled rolling maneuvers of a model in the wind tunnel was demonstrated using actively controlled (via digital control) leading- and trailing-edge control surfaces.

2) Torsion moment reduction was targeted as the design objective, and experimental evaluation of two RMLA controllers showed up to a 61.6% reduction in peak incremental torsion moments as compared to those generated by corresponding baseline rolling maneuvers at equivalent dynamic pressures having the same time-to-roll performance. Incremental bending moments, although not targeted for reduction, were evaluated and the resulting loads were well within load limit margins for both RMLA controllers.

3) Control law B, using a pair of leading-edge control surfaces showed at least 14% greater reduction capability of the outboard torsion moment than control law A using trailing-edge surfaces, while achieving a minimum 31% reduction in inboard incremental torsion moment relative to a baseline rolling maneuver. This was achieved with less than a 2% increase in peak incremental bending moments relative to static load limits. These results show that LEO control surfaces may be more effective for reducing outboard torsion loads during rolling maneuvers than TEO controls.

4) It was demonstrated by experiment that the RMLA and flutter suppression control laws could operate effectively together during rolling maneuvers 11% above the critical open-loop flutter dynamic pressure.

References

[1]O'Connell, R. F., "Design, Development and Implementation of an Active Control System for Load Alleviation for a Commercial Transport Airplane," 49th Meeting of the AGARD Structures and Materials Panel, Cologne, Germany, Oct. 1979.

[2]Rollwagen, G., Ellgoth, H., and Beuck, G., "Identification of Dynamic Response, Simulation and Design of a Highly Nonlinear Digital Load Alleviation System for a Modern Transport Aircraft," 17th Congress of the International Council of the Aeronautical Sciences, Stockholm, Sweden, Sept. 1990.

[3]Sandford, M. C., Abel, I., and Gray, D. L., "Development and Demonstration of a Flutter-Suppression System Using Active Controls," NASA TR R-450, Dec. 1975.

[4]Noll, T. E., and Huttsell, L. J., "Wing Store Active Flutter Suppression—Correlation of Analyses and Wind-Tunnel Data," *Journal of Aircraft*, Vol. 16, No. 7, 1979, pp. 491–497.

[5]Rogers, K. L., Hodges, G. E., and Felt, L., "Active Flutter Suppression—A Flight Demonstration," *Journal of Aircraft*, Vol. 12, No. 6, 1975, pp. 551–556.

[6]Sensburg, O., Honlinger, H., Noll, T. E., and Huttsell, L. J., "Active Flutter Suppression of an F-4F Aircraft," *Journal of Aircraft*, Vol. 19, No. 5, 1982, pp. 354–359.

[7]Miller, G. D., "Active Flexible Wing (AFW) Technology," Air Force Wright Aeronautical Labs., AFWAL TR-87-3096, Feb. 1988.

[8]Perry, B., Cole, S. R., and Miller, G. D., "A Summary of the Active Flexible Wing Program," AIAA Paper 92-2080, April 1992.

[9]Reed, W. H., III, Foughner, J. T., Jr., and Runyan, H. L., Jr., "Decoupler Pylon: A Simple, Effective Wing/Store Flutter Suppressor," *Journal of Aircraft*, Vol. 17, No. 3, 1980, pp. 206–211.

[10]Hoadley, S. T., and McGraw, S. M., "The Multi-Input/Multi-Output Multi-Function Digital Controller System for the AFW Wind-Tunnel Model," AIAA Paper 92-2083, April 1992.

[11]Perry, B., Dunn, H. J., and Sandford, M. C., "Control Law Parameterization for an Aeroelastic Wind-Tunnel Model Equipped with an Active Control System and Comparison with Experiment," NASA TM-100593, April 1989.

[12]Etkin, B., *Dynamics of Flight*, Wiley, New York, 1959.

[13]Woods-Vedeler, J. A., Pototzky, A. S., and Hoadley, S. T., "Active Load Control During Rolling Maneuvers," NASA TP-3455, Oct. 1994.

[14]Mukhopadhyay, V., and Newsom, J. R., "A Multiloop System Stability Margin Study Using Matrix Singular Values," *Journal of Aircraft*, Vol. 7, No. 5, 1984, pp. 582–587.

[15]Mukhopadhyay, V., "Flutter Suppression Digital Control Law Design and Comparison with Experiment for the AFW Wind-Tunnel Model," AIAA Paper 92-2095, April 1992.